Characterization of single functionalized quantum dots using combined atomic force and confocal fluorescence microscopy

Dal-Hyun Kim[a], Kenji Okamoto[b], Lori S. Goldner, and Jeeseong Hwang*

National Institute of Standards and Technology, Physics Laboratory, Optical Technology Division, 100 Bureau Drive, Mail Stop 8443, Gaithersburg, MD 20899 USA
[a] Present address: Nanosurface Group, Korea Research Institute of standards & Science, Daejeon, 305-340 Korea
[b] Present address: Department of Chemistry, Graduate School of Science, Kyoto University, Kyoto, 606-8502 Japan

ABSTRACT

Fluorescent nanocrystals (quantum dots or QDs) have a number of unique properties that overcome the limitations of conventional organic dyes. However, the optical properties of QDs have been observed to be strongly dependent upon their local chemical environment including novel surface coatings, which have been developed to render QDs water soluble and conjugation ready leading to their use as fluorescent tags and optical sensors for a variety of biological and biomedical applications. The quantitative utility of QDs in complex biological systems requires that their optical properties be well understood and interrelated with their chemical functionalization on the surface and their interactions with surface-conjugated materials. In this report, quantitative measurement of adhesion forces between a hydrophilic or a hydrophobic AFM probe and an amine-functionalized single QD or a hydrophilic substrate were obtained to demonstrate the utility of the atomic force microscopy (AFM) as a tool to probe surface functionalities of single functionalized QDs. We also present procedures to combine AFM and confocal fluorescence microscopy in an effort to simultaneously probe optical characteristics and physical/chemical properties of single or clustered functionalized QDs at the nanoscale.

Keywords: single nanocrystal, confocal microscope, atomic force microscope, quantum dot

1. INTRODUCTION

Conventional fluorescent bio-labeling markers involve organic fluorescent molecules and protein complexes including fluorescently tagged antibodies and macromolecules integrated with a genetically expressed fluorescent moiety. While these conventional markers are sufficient for many applications, their broad application is ultimately limited by fast photo bleaching, broad emission spectra, and chemical instability. Fluorescent nanocrystals (quantum dots or QDs) have a number of unique fluorescent properties that overcome the limitations of conventional organic dyes: they exhibit long fluorescence lifetimes, narrow emission spectra, and are not susceptible to photodegradation.[1] QDs not only exhibit higher fluorescence quantum yields than organic dyes, but their longer fluorescence lifetime allows temporal "gating" with respect to background autofluorescence which is indispensable for biological imaging and sensing applications. Only a few nanometers in diameter, QDs in this study are composed of a semiconductor core of Cadmium Selenide (CdSe) capped with a Zinc Sulfide (ZnS) shell. CdSe/ZnS QDs fluoresce with a very broad absorption and narrow emission spectra. By adjusting the core size, the emission wavelength can be finely tuned. The ZnS shell helps in stabilizing the core, makes the light emission more intense, and keeps the QD from degrading. For biological applications, recent studies demonstrate that the surfaces of CdSe/ZnS QDs can be conjugated with biological molecules (such as proteins, lipids, DNA, and RNA), so they can be readily incorporated into specific sites of complex biological and biomimetic systems for *in vivo* and *in vitro* imaging applications.

Despite the excellent photochemical and physical properties described above, the fluorescent properties of QDs have been observed to be strongly dependent upon their local physical and chemical environment. For example, early

Colloidal Quantum Dots for Biomedical Applications, edited by Marek Osinski, Kenji Yamamoto, Thomas M. Jovin,
Proc. of SPIE Vol. 6096, 60960G, (2006) · 0277-786X/06/$15 · doi: 10.1117/12.661784

studies revealed that the electronic states of QDs are very susceptible to surface defects and adatoms, which can induce massive changes in QD fluorescent properties, such as spectral shifts, fluorescence intermittency (or blinking), and fluorescence intensity variations.[2] Additionally, the fluorescent properties of single CdSe/ZnS QDs have been found to be dependent upon the local chemical environment in which the QDs are contained or the surface functionalization which may induce deep trap states responsible for long time period non-emissive states.[3,4] Much effort in the development of proper surface functionalization has been made to lessen the blinking phenomenon or produce optically stable QDs. To understand how surface conjugation influences optical characteristics of QDs at the nanoscale, detailed assessment of surface functionalization properties to interrelate them with fluorescent characteristics at the single QD level is a key.

Recently, single molecule fluorescence microscopy has been widely employed to measure fluorescence properties of single bio-conjugated QDs to understand how their surface functionalities influence their optical properties.[4] Since the spatial resolution of fluorescence microscopy is diffraction-limited, the addition of atomic force microscopy (AFM) allows complementary physical characterization of QDs including qualitative characterization of surface functionalization. A functionalized AFM probe, modified with well-defined, specific surface functional groups (e.g., -CH_3, -NH_2, -COOH, -OH) at the probe tip, may produce specific probe/surface interactions (e.g., adhesion force) that reflect the probe chemistry and the local chemistry of the sample surface.[5] Approaches to combine AFM and confocal fluorescence microscope to probe nanoscale bio-conjugated materials (e.g. nanospheres) have been demonstrated by others for a variety of bio-nanotechnology applications.[6] For instance, single fluorescent polystyrene nanospheres and fluorescently labeled DNA molecules were studied on mica using combined time-resolved confocal fluorescence microscopic spectroscopy and AFM,[7] and the conformational dynamics of grana membranes in plant chloroplasts was revealed using dye-loaded latex beads in the platform of two-photon fluorescence microscopy combined with AFM.[8] However, combined functionalized AFM and confocal fluorescence microscopy has not previously been employed for the characterization of the functional groups of water-soluble single QDs. Here, we report our progress on the technical development of combined confocal and atomic force microscopy as a measurement tool in an effort to quantitatively interrelate fluorescence properties with surface-functionalization of single QDs. In the process, we develop a combined chemical force/confocal optical microscope that has broad applications towards nanoscale metrology of bio-conjugated luminescent materials.

2. METHODOLOGIES

2.1 Sample and AFM tip preparation

QD samples were prepared on clean borosilicate glass cover slips (No. 1.5, Corning). Prior to use, the cover slips were cleaned in a piranha solution (100% H_2SO_4 : 30% H_2O_2, 3:1 volume) for 24 hours, rinsed copiously with 18.2 Mohm water (Barnstead). The cover slips were dried by nitrogen gas, followed by 20 minutes of ultraviolet-ozone cleaning (Jelight) resulting in OH-rich, hydrophilic surfaces. Amine- or carboxyl-functionalized CdSe/ZnS QDs (Fort Orange Type, 598 nm ± 10 nm emission, Evident Technologies) were spin-coated on the surface, following dehydration at 120 Degree C for 1 hour in a convection oven. For AFM topographic measurements, silicon AFM probes (CSC12, MikroMasch) were used. To achieve a hydrophilic probe surface the silicon tip was piranha-etched using a method described elsewhere [9] followed by dehydration of the tip surface at 150 Degree C for 2 days in a convection oven.

2.2 Simultaneous force curve and fluorescence measurement

From a topography image obtained in a non-contact mode, the coordinates of individual QDs were recorded and employed to position the probe at the center of each QD for further adhesion force measurement. To prevent a hard crash of the probe during the force curve acquisition, the z offset is incrementally added to approach the probe to the sample surface while repeating force curve measurements until the surface interaction is detected in the force curve. The adhesion force was calculated using k = 0.08 N/m, the probe's force constant provided by the manufacturer. The fluorescence photons were collected in a pulse counting mode by an Avalanche Photodiode (APD, SPCM-AQR-14, Perkin Elmer Optoelectronics) interfaced to the AFM data acquisition system (Asylum Research) using a data acquisition interface board (PCI6111, National Instrument). Igor-based software routines were developed to simultaneously collect a 2D fluorescence confocal image and an AFM topographic image in a raster X,Y scan mode and a force curve and the fluorescence emission as function of the probe position from the sample surface.

2.3 Confocal fluorescence microscopy

A schematic of the combined AFM and confocal fluorescence microscope is illustrated in Figure 1(A). The optical train of the light for confocal fluorescence detection is given in the following. A 488 nm excitation beam from a CW solid state laser (Sapphire 488-20 CDRH, Coherent) is reflected by a 2-axis piezo scanning reflecting mirror (used to align the excitation laser spot to the end of an AFM probe as describe below), passed through a 488 nm bandpass filter and a 515 nm long-pass dichroic mirror (515 DRLP, Omega Optical) mounted at 45 degree relative to the optical axis of an oil-immersion objective lens (60X, 1.45NA, Olympus Microscope) focusing the light onto the upper surface of a No. 1.5 glass cover slip. The laser power incident on the dichroic mirror was 2.8 μW. The fluorescence emission is back collected from the same objective lens, the dichroic mirror, and a set of a 488 notch filter (Kaiser Optics), two short pass filters (750SP and 700SP) to reject the scattering from a AFM diode laser, and a band pass filter (590DF35, Omega Optical). The photon counting of the emission was performed using an APD which is mounted on a 3-axis mechanical translator to adjust its position to align the focused fluorescence emission onto an active area (175 μm diameter) of the APD.

2.4 Alignment of a confocal beam onto the apex of an AFM probe.

We developed a technique to precisely align a focused excitation laser spot onto the AFM probe tip (Figure 1B). Light from the 488 nm laser travels through a polarizing beam splitter and is then focused through a confocal pinhole. A two-axis piezo-stacked mirror (Nano-Drive, Mad City Labs, Inc) is used to raster-scan a laser beam spot over a sample surface to find the tip position of an AFM probe maintained close to the sample surface by employing tapping mode feedback. A 1:1 telescope is used to transfer an image of the scanning mirror into the back focal plane of the objective, which facilitates scanning. A quarter wave plate just before the microscope is used to adjust the polarization of light reflected from the surface to be perpendicular to incoming light. This reflected light therefore is diverted into the photodiode at the polarizing beam-splitter. Using the photodiode, we construct a 2D image of the scanned area. In the image, maximum reflection was observed at the position when the focused laser spot illuminates the sample position where our silicon AFM probe touches the surface. Alignment of the confocal beam onto the probe end was achieved by applying the offset voltages to the mirror to keep the laser spot at the AFM tip while AFM images were obtained.

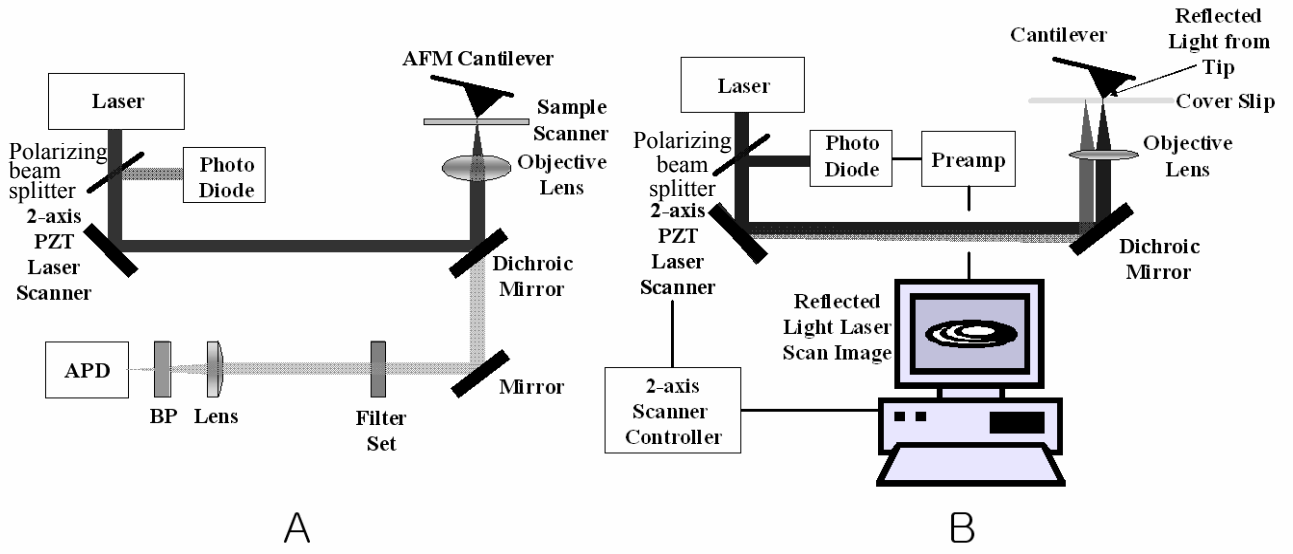

Figure 1. (A) A schematic of atomic force microscope combined with confocal fluorescence microscope. (B) A schematic to align a focused excitation laser beam onto the end of an AFM probe. A 2-axis laser scanner was used to raster scan a focused beam over the surface of a glass coverslip and a photodiode to detect the reflected back-scattered laser beam from the sample surface and the AFM probe close to the surface. The de-scanned back-scattered beam is detected through a confocal pinhole. The optics used to relay the scanning mirror into the back focal plane of the objective are not shown.

3. RESULTS and DISCUSSION

Figure 2(A) is a typical AFM topography image of amine-functionalized QDs spin-coated onto a clean hydrophilic glass cover slip. A silicon AFM probe was used to obtain the images in Figure 2. Provided that all the QDs are functionalized with the same surface coating with amine functional end groups, we would expect the size of single QDs to be uniform. Instead, a broad bimodal distribution of topographic heights is observed (Figure 2A). The two peaks were evident at approximately 4.5 nm and 8.5 nm (two arrows in Figure 2B). The large (truncated) peaked at 0 nm represents the fluctuations in the substrate height. The peak near 4.5 nm is consistent with what would be expected from bare, unfunctionalized QDs (data not shown) implying that some QDs may have lost their surface coating. The mean local height of the smaller QDs, measured by taking topographic profiles of each smaller particle, was 5 nm ± 1 nm, which is close to the theoretical value for bare Fort Orange QDs, 6.3 nm. For the larger particles, an average height of 14 nm ± 2 nm was obtained , which we believe to be the size of amine-functionalized QDs.

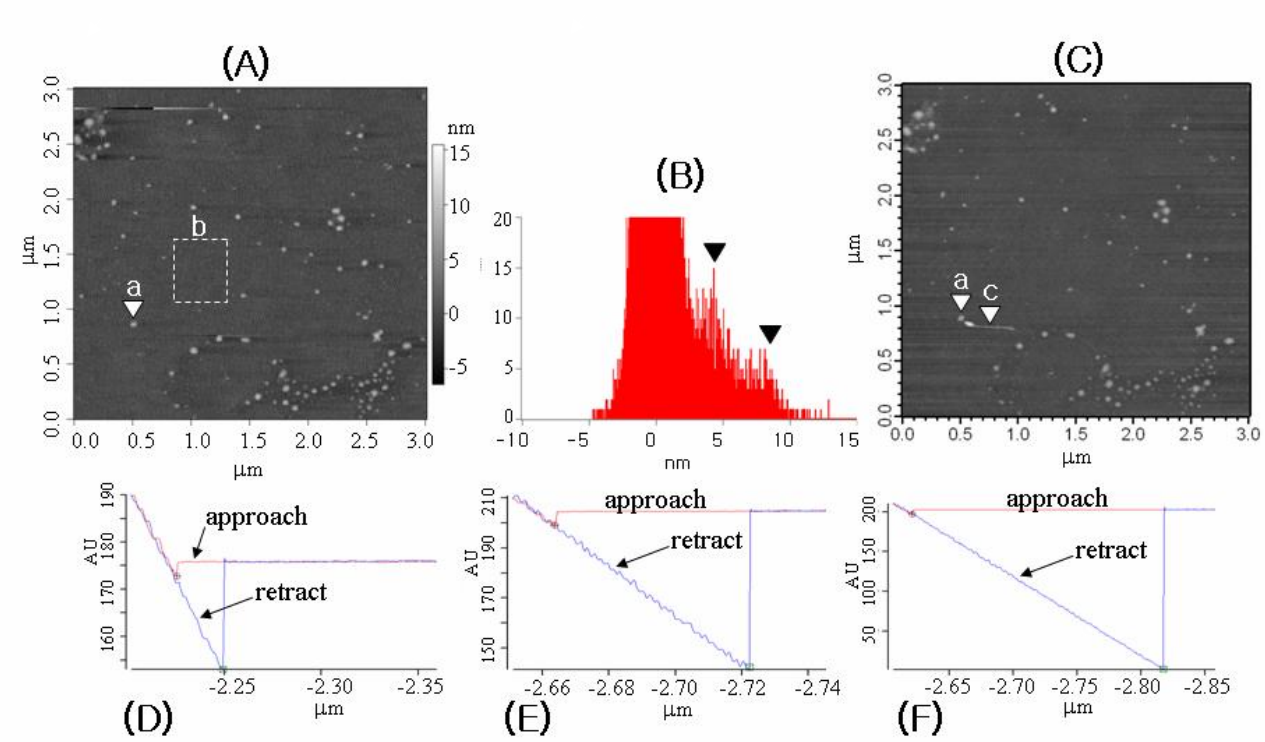

Figure 2. The AFM topography image before (A) and after (C) the detachment of amine coated quantum dot(s) from an untreated silicon AFM tip. Image size is 3.01 µm x 3.01 µm. In C, a new feature (arrow pointing down) appeared which is believed to be amine-functionalized QD(s) dragged by the AFM tip before getting fixed onto the substrate surface. Force curves between the tip and the amine coated QD(a) before (D) and after (E) the detachment of amine coated quantum dot(s) from the AFM tip. The adhesion force increased from 1.2 nN to 4.8 nN after obtaining the image C. (F) A force curve measured on the hydrophilic substrate area (region b in Fig.A) at the time between the two images, resulting in 15.7 nN, significantly larger than two other cases. Adhesion forces were calculated by multiplying *k*, the force constant of the tip, and the distance between the surface contact point (local minimum point at the approaching curve) and the release point (minimum in the retract curve) of the tip.

The average adhesion force initially measured between the silicon probe and the surfaces of several different large particles, presumably amine-functionalized QDs, was 5.0 nN ± 0.5 nN (all the tolerance values presented in this paper are for 1 standard deviation). During the repetition of several scans of this QD sample, we occasionally observed that an AFM tip picks up and deposits some unknown number of particle(s), possibly bare or functionalized QDs, from or onto the substrate surface. This is probably due to weak non-covalent attachment of QDs to the glass surface or to the probe

surface. Accordingly, the chemical property of the AFM end is found to evolve resulting in changes in the adhesion forces when measured over the same sample spots. For instance, after obtaining several topographic images of the sample area of QDs as shown in Figure 2(A), the mean adhesion force measured over an amine-functionalized QD (the particle "a" in Figures 2A and 2C) decreased to 1.2 nN. Further adhesion force measurements were performed on 10 different larger particles to obtain the mean value of 1.4 nN ± 0.5 nN. However, the tip became more hydrophobic over time, possibly from collecting either hydrocarbon contaminants or amine-functionalized QDs from the surface. Our results below seem to indicate that amine-functionalized QDs are the likely culprits. In the topography image of Figure 2C, a new feature appeared (see the arrow "c"), which appears to be particle(s) detached from the tip, dragged by the tip along the surface, and fixed onto the substrate. After obtaining this topography image, adhesion forces were measured over the particle "a" to obtain 4.8 nN, which is close to the value initially measured by employing a bare silicon AFM probe. It is noteworthy that the adhesion force increased from 1.2 nN to 4.8 nN after obtaining the image C indicating that the tip became more hydrophilic after losing the particle (Figure D and E respectively). During the time period between taking the two images of Figure 2A and 2C, we also measured the adhesion force over random spots of the QD-free regions of the cover slip (region b in Figure 2A). The average value of 14.7 nN ±1.1 nN was obtained over the random spots. Figure 2F displays a typical force curve of this measurement gauging 15.7 nN, significantly larger than the previous two cases presumably involving amine-amine interaction (D) and amine-silicon interaction (E). The increased force value is indicative of stronger adhesion due to increased hydrophilicity of the hydroxyl-rich substrate.

From the above results, we speculate that the evolution of the AFM probe's hydrophobicity may be the result of amine-functional groups of QD(s) attached onto the AFM probe in the course of scanning. For more conclusive evidence, we piranha-etched the same probe and compared the adhesion forces between amine-functionalized QDs and the –OH rich probe with the forces obtained between an "amine-functionalized (by attaching amine-coated QDs)" AFM probe and the piranha-etched –OH rich glass substrate. Not surprisingly, we obtained 15.5 nN ± 0.8 nN as the force between piranha-etched tip and amine-functionalized QDs, which is similar to the result (14.7 nN ± 1.1 nN) measured between an "amine-functionalized" AFM probe and a piranha etched glass substrate. After the force measurements on amine-functionalized QDs, the same piranha-etched tip was used to assess adhesion forces on random spots of a QD-free region of the hydrophilic cover slip surface to obtain 18.4 nN ± 0.7 nN. This result is consistent with our expectation that the –OH (on the tip) and –OH (on the substrate) provides an even more hydrophilic interaction.

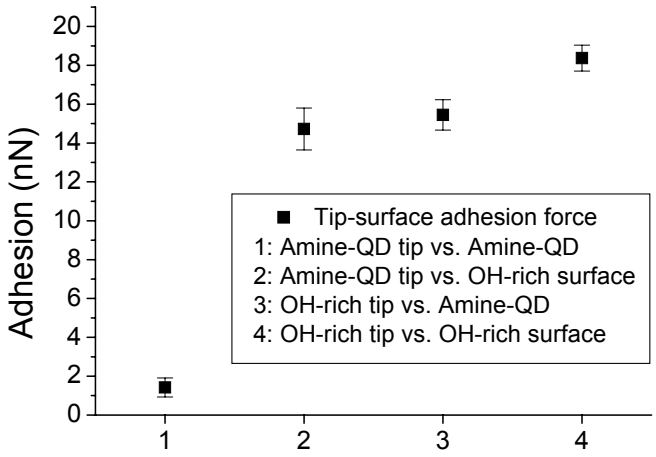

Figure 3. The adhesion force between 4 different combinations of tips and surfaces.

A capillary force is a dominant interaction between the tip and the surface in ambient AFM measurements, which is determined by the hydrophilicity or hydrophobicity of surface and tip.[10] More quantitatively, the equation of capillary adhesion between the sample surface and an AFM probe can be estimated with an equation:

$$F = 4 \pi R \gamma_L \cos\theta$$

where R is the radius of the sphere, γ_L is the interfacial energy of water in air, and θ is the water contact angle of the surface and sphere, respectively.[11] The contact angle of a piranha etched (OH-rich) and the amine-functionalized surface have been measured to be 24 º ($\cos\theta \approx 0.91$) and 65 º - 80 º ($\cos\theta \approx 0.17$ - 0.42) respectively,[12-14] suggesting that the capillary force between the OH-rich substrate and a –OH rich sphere is 2-5 times larger than that of the amine-amine interaction case, and amine-OH interaction will result in the intermediate value. Our measured adhesion forces qualitatively agree with the expectation according to this model. Moreover, the similarity in the adhesion forces in two cases, e.g. (1) between a piranha-etched probe and amine-functionalized QDs and (2) between a piranha-etched substrate

and the probe coated with "particles", supports our assertion that the coated particles on the probe are amine-functionalized QDs. The adhesion forces measured in the above 4 different cases (between hydrophobic or hydrophilic probe and hydrophobic or hydrophilic substrate) are summarized in Figure 3.

Taking advantage of our optical and AFM alignment capabilities, we can obtain fluorescent properties of single functionalized QDs and interrelate them with AFM force measurements on the same QD. Figure 4A is a typical reflection image of a blank glass cover slip with an AFM probe maintained close to the substrate surface with intermittent force ("tapping mode") feedback. When the raster scanned laser spot illuminates the position where AFM probe intermittently contacts the surface, the reflected light intensity is maximized. A higher resolution image of the tip region is shown in Figure 4B, which is a 3D representation of a 2D reflection image. The bright feature in the image is the AFM tip. The full width of the half maximum (FWHM) of the bright spot in Figure 4B, is 0.28 μm (12 pixels). Assuming that the maximum backscattering is obtained when the Gaussian peak of the focused laser beam is aligned at the apex of the AFM probe, we estimate a positioning accuracy of the confocal beam can be achieved at 23 nm or better under these conditions. For ultimate positioning accuracy of the focused beam, more rigorous modeling will be necessary to deconvolve the tip geometry from the optical image and take into account the profile of the optical field. Nevertheless, we discovered the patterns that the bright spot produces proves to be useful information regarding the quality of AFM probes. Contaminated tips show multiple bright spots, and blunt tips make much broadened patterns, both of which can be confirmed by topography images taken using compromised tips (data not shown).

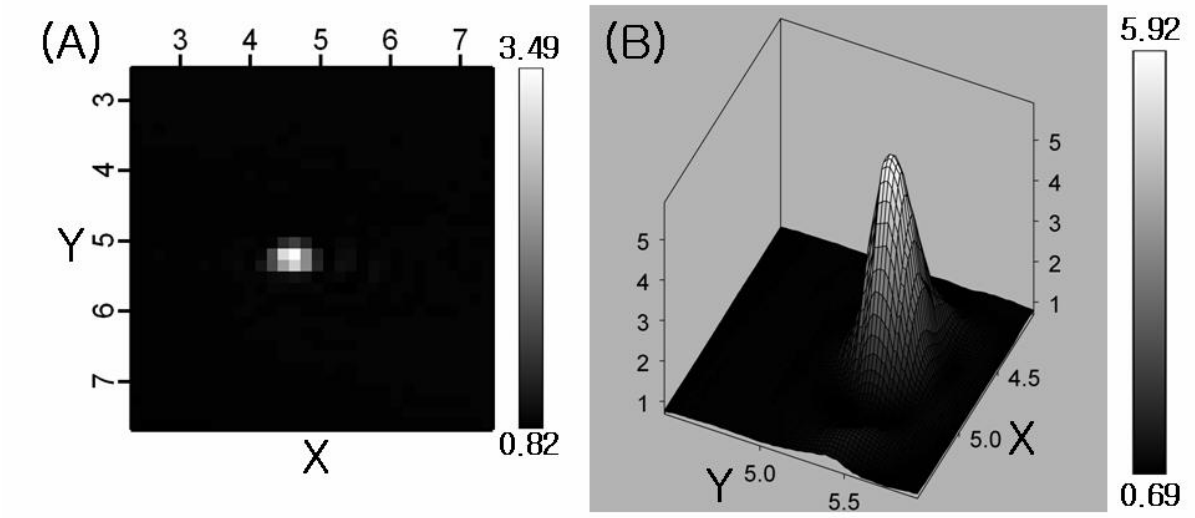

Figure 4. Reflected light laser scan images of an AFM tip, larger area (A) of 32 x 32 pixels equivalent to 4.45 μm x 5.83 μm and smaller area (B) 3D reconstructed image of the reflection intensity of 64 x 64 pixels equivalent to 1.26 μm x 1.54 μm. The scales in X and Y represent the voltages in V applied to a 2-axis PZT laser scanner, and vertical scale bar represents the voltage in V measured from a photodiode. The end of the AFM tip close to the surface in tapping mode feedback reflected more laser beam and contributed the brighter spot in the image.

Figure 5(D) is a topography only image of carboxyl-functionalized QDs on a glass substrate. After obtaining this image, the alignment of the confocal beam to the end of an AFM probe was accomplished according to the procedures described above, and the sample stage was raster scanned to simultaneously obtain fluorescence (Figure 5A) and topography (Figure 5B) images (256 x 256 pixels, 948 nm x 948 nm) of the selected area (shown as a square in Figure 5D). Data were obtained at 0.23 Hz per line scan for the topography and with 6.8 ms photon integration time per pixel for the fluorescence detection. By comparing these images, pixel to pixel comparison became possible to precisely interrelate optical and topographic characteristics of the QDs at the nanoscale. We noticed that the positions of QDs in both images coincide quite well confirming the alignment is well established. The two imaging modalities complement

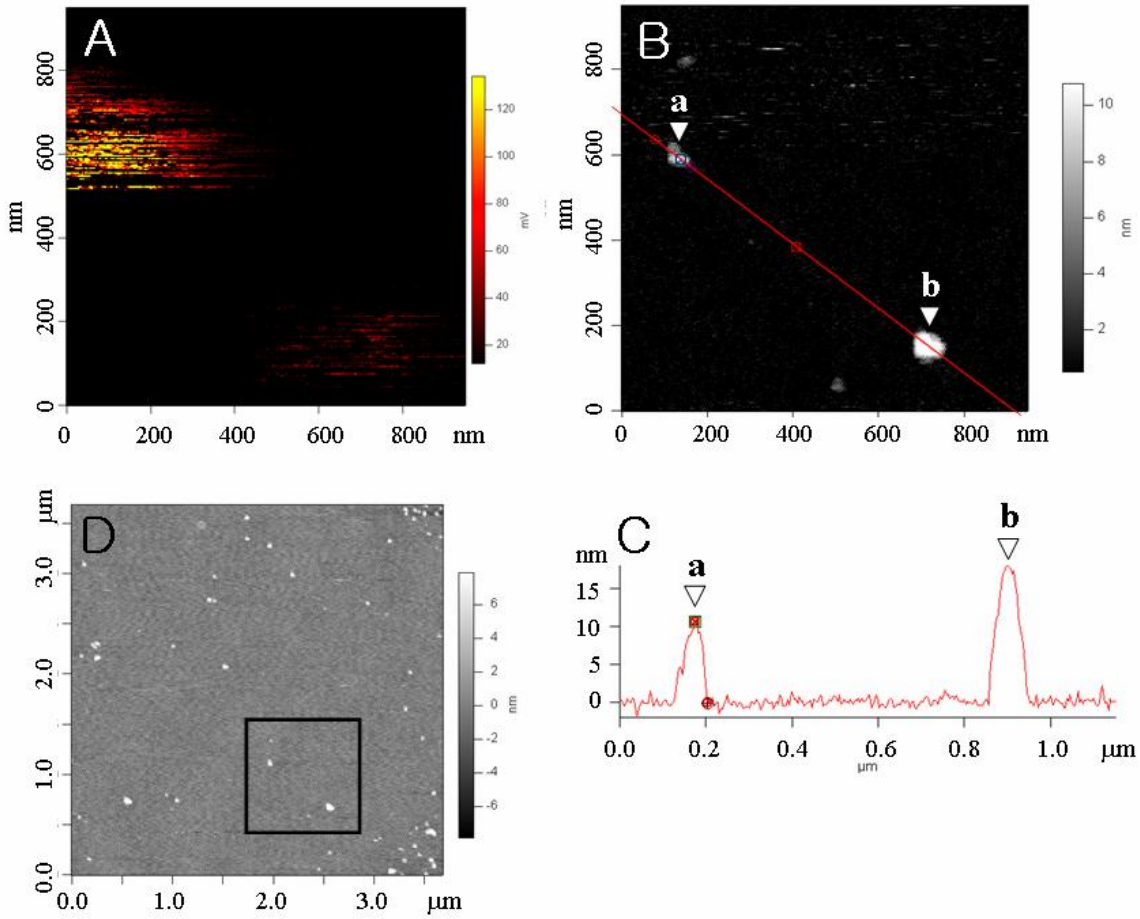

each other allowing unambiguous characterization of single QDs. For instance, the size (≈ 10nm) information from the

Figure 5. (A) Confocal fluorescence image and (B) AFM topography image of carboxyl-coated QDs on a cover slip of the selected area of the area shown in (D). (C) A topographic profile along the red line in (B). 1mV of the scale bar in (A) corresponds to 147 counts/s in photon counting.

topography image and the "blinking" fluorescence emission from the confocal image elucidated that the smaller feature ("a" in Figure 5B) in Figure 5 is a single functionalized QD. On the other hand, the larger feature (b in Figure 5B) appears to be an aggregate of QDs and yet exhibits much weaker fluorescence emission. Further exploration on the interrelationship between optical characteristics such as fluorescence spectra, intensity, and blinking and a variety of physical and chemical properties of QDs such as surface functionalities and degree of aggregation is in progress.

4. CONCLUSION

We have reported adhesion forces between an AFM probe and the surface of functionalized substrates or single functionalized QDs. As expected, the effect of surface functionalities was demonstrated to have a large effect on the adhesion forces. The maximum adhesion force was obtained between a piranha-etched AFM probe and the surface of a piranha-etched glass substrate. In addition, we developed a combined technique of fluorescence microscopy and atomic force microscopy and demonstrated its capability to simultaneously measure optical and force characteristics of single functionalized QDs. We presented simultaneously obtained AFM topography and confocal fluorescence images of a

sub-micrometer area of substrate supporting carboxyl-functionalized QDs and in the process demonstrated the precise alignment of the confocal beam with the tip end of an AFM probe. This technique will provide fundamental understanding on how the surface functionalization affects the optical properties of bio-conjugated photoluminescent nanocrystals such as QDs and nanoshells. This method may also be utilized to assess, employ, and manipulate the optical and physical/chemical properties of other biophotonic nanomaterials for their best utilities.

5. ACKNOWLEDGEMENT

Authors thank Drs. John Woodward, Kimberly Briggman, and Peter Yim for useful discussions. JH was supported by the National Institute of Standards and Technology Advanced Technology Intramural Program. DHK was partly supported by the Korea Research Foundation Grant (KRF-2004-214-C00169) supported by MOEHRD and Nanobio Measurement and Manipulation Project supported by MOCIE, Korea. Certain commercial equipment, instruments, or materials are identified in this paper to foster understanding and does not imply recommendation or endorsement by NIST, nor does it imply that the materials or equipment identified are necessarily the best available for the purpose.

6. REFERENCES

1. X. Michalet, F. F. Pinaud, L.A. Bentolila, J. M. Tsay, S. Doose, J. J. Li, G. Sundaresan, A. M. Wu, S. S. Gambhir, S. Weiss, "Quantum dots for live cells, in vivo imaging, and diagnostics", *Science*. **307**, 538 (2005).
2. A. P. Alivisatos, "Semiconductor clusters, nanocrystals, and quantum dots", *Science*. **271**, 933 (1996).
3. F. Koberling, A. Mews, T. Basche, "Oxygen-induced blinking of single CdSe nanocrystals", *Advanced Matererials.* **13**, 672 (2001).
4. J. Yao, D. R. Larson, H. D. Vishwasrao, W. R. Zipfel, W. W. Webb, "Blinking and nonradiant dark fraction of water-soluble quantum dots in aqueous solution," *Proceedings of the National Academy of Sciences of the United States of America*. **102(40)**, 14284–14289, 2005.
5. J-B D. Green, A. Idowu, S. S. F. Chan, "Modified tips: molecules to cells," *Materials today*, **6(2)**, 22 (2003).
6. R. Kassies, K. O. van der Werf, A. Lenferink, C. N. Hunter, J. D. Olsen, V. Suramaniam, C. Otto, "Combined AFM and confocal fluorescence microscope for applications in bio-nanotechnology", *Journal of Microscopy*. **217**, 109 (2005).
7. L. A. Kolodny, D. M. Willard, L. L. Carillo, M. W. Nelson, A. van Orden., "Spatially correlated fluorescence/ AFM of individual nanosized particles and biomolecules", *Analytical Chemistry*. **73**, 1959 (2001).
8. C. C. Gradinaru, P. Martinsson, T. J. Aartsma, T. Schmidt., "Simultaneous atomic-force and two-photon fluorescence imaging of biological specimens in vivo", *Ultramicroscopy*. **99**, 235 (2004).
9. P. Hinterdorfer, W. Baumgartner, H. J. Gruber, K. Schilcher, H. Schindler, "Detection and localization of individual antibody-antigen recognition events by atomic force microscopy", *Proceedings of the National Academy of Sciences of the United States of America*. **93**, 3477 (1996).
10. W. F. Heinz, J. H. Hoh, "Spatially resolved force spectroscopy of biological surfaces using the atomic force microscope", *Nanotechnology*. **17**, 143 (1999).
11. J. N. Isrelachvili, *Intermolecular and Surface Forces*, (Academic Press, London, 1992), p. 332.
12. L. D. Eske, D. W. Galipeau, "Characterization of SiO_2 surface treatments using AFM, contact angles and a novel dewpoint technique", *Colloids and Surfaces A: Physicochemical and Engineering Aspects*. **154,** 33 (1999).
13. N. Faucheux, R. Schweiss, K. Ltzkow, C. Werner, T. Groth, " Self-assembled monolayers with different terminating groups as model substrates for cell adhesion studies ", *Biomaterials*. **25**, 2721 (2004).
14. M. Ranckl, S. Laib, S. Seeger, "Surface tension properties of surface-coatings for application in biodiagnostics determined by contact angle measurements ", *Colloids & Surfaces B: Biointerface.* **30**, 177 (2003).

*jch@nist.gov; phone 1 301 975-4580; fax 1 301 975-6991